Histochemical structure and tensile properties of birch cork cell walls

Shingo Kiyoto[1] • Junji Sugiyama*[1,2]

[1] Laboratory of Tree Cell Biology, Division of Forest and Biomaterials Science, Graduate School of Agriculture, Kyoto University, Sakyo-ku, Kyoto 606-8502, Japan

[2] College of Materials Science and Engineering, Nanjing Forestry University, Nanjing, 210037 China

* Corresponding author: Junji Sugiyama

e-mail: sugiyama.junji.6m@kyoto-u.ac.jp

Phone: +81-75-753-6240

ORCID-ID: https://orcid.org/0000-0002-5388-4925

Abstract

Tensile tests of birch cork were performed in the tangential direction. Birch cork in the wet state showed significantly higher extensibility than those in the dried state. The histochemical structure of birch cork was investigated by microscopic observation and spectroscopic analysis. Birch cork cell walls showed a two-layered structure and the inner material bordering cell wall. In transmission electron micrographs, osmium tetroxide stained the outer layer and inner material, whereas potassium permanganate stained the inner layer and inner material. After removal of suberin and lignin, only inner layer remained and Fourier-transformed infrared spectra showed the cellulose I pattern. Polarizing light micrographs indicated that molecular chains in the outer layer and inner material were oriented perpendicular to suberin lamination, whereas those in the inner layer showed longitudinal orientation. These results suggested that the outer layer and inner material mainly consist of suberin, whereas the inner layer and compound middle lamella consist of lignin, cellulose, and other polysaccharides. We hypothesized a hierarchical model of the birch cork cell wall. The lignified cell wall with helical arrangement of cellulose microfibrils is sandwiched between suberized outer layer and inner material. Cellulose microfibrils in the inner layer bear tensile loads. In the wet state, water and cellulose transfer tensile stress. In the dried state, this stress-transferal system functions poorly and fewer cells bear stress. Suberin in the outer layer and inner material may prevent absolute drying to maintain mechanical properties of the bark and to bear tensile stress caused by trunk diameter growth.

Keywords Cellulose, Cork, Polarizing light microscopy, Suberin, Transmission electron microscopy

Abbreviations

FTIR Fourier-transformed infrared

$KMnO_4$ potassium permanganate

OsO_4 osmium tetroxide

PAS periodic acid–Schiff

PLM polarizing light microscopy

TEM transmission electron microscopy

Declarations

Funding

This research was financially supported by Grants-in-Aid for Scientific Research on Innovative Areas (18H05485).

Conflicts of interest/Competing interests

There is no conflict of interest.

Availability of data and material

Data sharing is not applicable to this article.

Authors' contributions

JS conceived and designed research. SK conducted experiments and wrote the manuscript. All authors read and approved the manuscript.

Introduction

Cork is the outermost tissue of the bark and plays an important role in protecting the tree body owing to its thermal insulation, pest resistance, and water repellency. To confer these properties, cork cell walls have a distinct chemical constitution and anatomical structure from those of other tissues. The most important characteristic of the cork cell wall is a high content of suberin. Suberin is an aliphatic-aromatic crosslinked polyester (Gardini et al. 2006). Several properties of cork, such as thermal stability, originate from the presence of suberin (Pereira 2015). Cork from a number of woody species has been used for its useful properties. Mechanical properties of cork differ among tree species because of differences in anatomical structure and results in different industrial usages.

The most popularly used cork is that from Quercus suber. It has been used as a bottle stopper on account of its low density, impermeability to water and gases, high compressive strength, and dimensional recovery. These properties reflect the cell size and structure of the hexagonal prism (Gibson et al. 1981). Cherry cork has been used as a Japanese traditional craft ("Kabazaiku") such as tea-things, a papeterie and so on because of its smooth surface and beautiful glossy, dark red color. In addition, the mechanical properties of cherry cork are notable: extensibility greater than 120%, Young's modulus 0.9–1.6 GPa, and toughness approximately 40 MPa in the tangential direction (Kobayashi et al. 2018; Xu et al. 1997). These values surpass the tensile properties of Q. suber cork (Anjos et al. 2008; 2010). The tensile properties are due to the tangentially elongated cell shape and aligned cell wall fibers (Xu et al. 1997). In Russia, birch cork has been used as a traditional craft such as boxes, cylinder containers, caskets, dishes, chests and so on because of its toughness and water resistance. The anatomical structure and seasonal growth of birch cork has been investigated previously (Shibui and Sano 2018; Schönherr and Ziegler 1980; Bhat 1982). However, to the best of our knowledge, few studies have been conducted on the histochemical structure of the cell wall and the mechanical properties of birch cork for its limited industrial uses, despite the broad distribution of birch on the Eurasian continent.

In this report, we performed tensile tests and surveyed the histochemical structure of birch cork using polarizing light microscopy (PLM) and transmission electron microscopy (TEM). From the insights obtained from these experiments, we discuss the relationship between the histochemical structure and mechanical properties of the cell wall of birch cork.

Materials and Methods

Plant materials

Outer bark was stripped from a birch tree (Betula platyphylla) growing in national forests in Gifu prefecture on 20 June 2014. The diameter at breast height of the sampled tree was 26 cm. After air-drying the bark, and removing outer layers weathered, the innermost portion of the bark (100-300 μm thick) was stripped, and was subsequently subjected to tensile tests, spectroscopic analysis, and microscopic observation.

Tensile test

A dumbbell-type strip of bark, with the dimensions 5 mm (L) × 0.2 mm (R, calibrated with a micrometer for each sample) × 30 mm (T), was trimmed with a metal mold for the tensile test. The air-dried samples were kept conditioned at room temperature. A portion of samples were oven-dried at 120 °C overnight and returned to room temperature in a desiccator containing silica gel for 6 h. Some samples were hydrated by de-aeration in water. Tensile tests in tangential directions were performed on 10 specimens per sample, with span length 20 mm and crosshead speed 10 mm min^{-1}, with a testing machine (LSC-1, Tokyo Kouki, Tokyo, Japan).

Chemical treatment for removal of suberin and lignin

To observe the cellulosic material in the cork cell wall, suberin and lignin were removed by alkali ethanolysis and the Wise method, respectively.

Suberin was removed from some samples in accordance with the method reported by Ekman and Eckerman (1985) with slight modification: the samples were hydrolyzed with 0.5 N KOH in 90% ethanol at 80 °C for 2 h without stirring. After washing repeatedly in distilled water, the samples were subjected to delignification via sodium chlorite oxidation in water at pH 4.8 at 70 °C for 1 h. The products were washed repeatedly in distilled water. Fourier-transformed infrared (FTIR) spectra were obtained from samples for each procedure using a FTIR spectrometer (Frontier, Perkin-Elmer, Waltham, MA, USA). Samples before and after chemical treatment were subjected to pretreatments for microscopic observation.

Sample preparation for microscopic observation

Birch cork samples were cut into small blocks with the dimensions 2.5 mm (L) × 0.3 mm (R) × 5 mm (T). Some of the samples were stained en bloc with 1% osmium tetroxide (OsO_4) in 0.1 M phosphate buffer or with 1% aqueous solution of potassium permanganate ($KMnO_4$) in 0.1% sodium citrate for 2 h at room temperature, and washed repeatedly with distilled water. These blocks were dehydrated through an ethanol series (up to 99.5% ethanol). The blocks were embedded in Spurr's resin. Some blocks were substituted with xylene and embedded in paraffin. Some blocks after removal of suberin and lignin were substituted with propylene oxide and embedded in Epon812 resin.

Polarizing light microscopic observation

Radial and transverse sections (each 5 μm thick) were cut from cork samples embedded in Spurr's resin before and after chemical treatment as described above. To determine molecular chain orientation from the polarization color, sections without chemical treatment were bleached by sodium chlorite oxidation in water at pH 4.8 at 70 °C for 1 h. These sections were stained using the periodic acid–Schiff reaction (PAS). Sections from the samples after removal of suberin and lignin were observed without staining. Sections were mounted with Bioleit mounting medium (Oken-shoji, Tokyo, Japan) and observed with a PLM (BX53-P, Olympus, Tokyo, Japan) equipped with a digital camera (DP74, Olympus).

Transmission electron microscopic observation

Radial and transverse ultrathin (100 nm thick) sections were cut from blocks of untreated samples before embedding. In addition, samples embedded with Epon812 resin after removal of suberin and lignin were also cut into ultrathin radial sections. These sections were mounted on copper grids (300 mesh) and floated on a drop of 1 % aqueous solution of $KMnO_4$ in 0.1 % sodium citrate for 30 min at room temperature. Sections were washed with distilled water, dried, and observed at 80 kV with a TEM (JEM1400, JEOL, Tokyo, Japan). Samples that were embedded in Spurr's resin after staining with OsO_4 or $KMnO_4$ were also used to cut ultrathin radial sections and observed without post-staining.

Raman microscopic observation

Transverse 10-μm-thick sections were cut from paraffin-embedded blocks. Paraffin was removed from the sections with xylene, and xylene was substituted to 100% ethanol. The sections were hydrated in a graded ethanol series until water was used. The sections were mounted on glass slides in distilled water, covered with cover glass, and sealed. The Raman spectra were acquired using a micro-Raman system (LabRam Xplora, Horiba Jobin Yvon, Essonne, France) equipped with a light microscope (BX51, Olympus) and laser (λ = 638 nm). The LabSpec instrumentation software (Horiba Jobin Yvon) was used to control the micro-Raman system. Baseline correction was performed based on the airPLS algorithm using Python 3.7.4 software (Zhang et al. 2017). Brightfield micrographs were also captured.

Results

Tensile tests

Wet-state birch cork showed the highest extensibility, followed in order by air-dried and oven-dried cork (Fig. 1a). Wet-state cork showed a lower elastic modulus than cork samples in the other two states and a significantly lower tensile strength than air-dried cork (Fig. 1b). Oven-dried cork showed lower toughness than samples in the other two states.

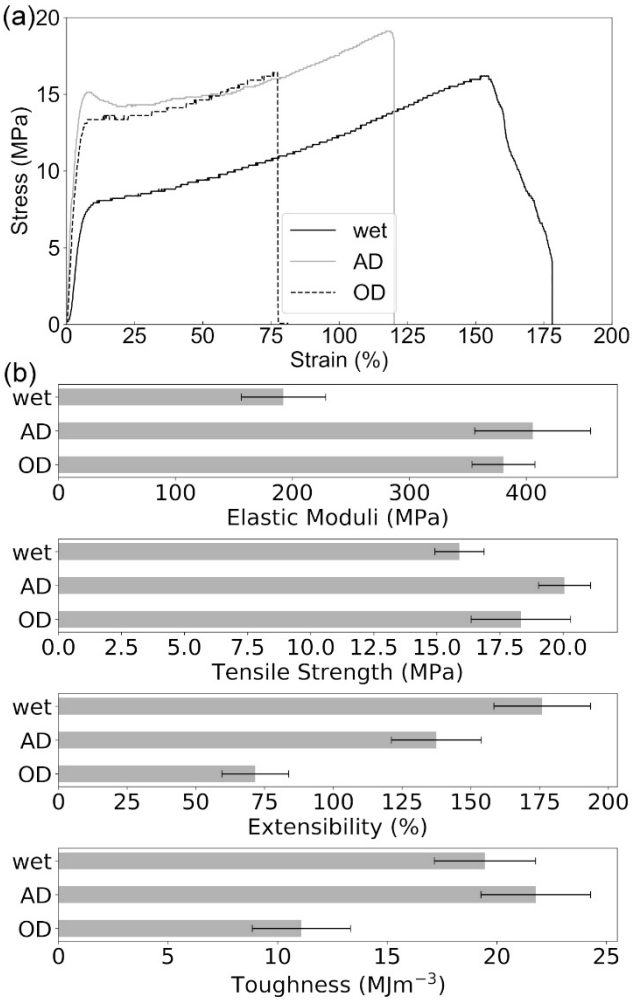

Fig. 1 Representative stress-strain curves of tensile tests in the tangential direction of wet-state, air-dried, and oven-dried birch cork (a), and mean value of each tensile parameter (b). Error bars indicate the standard deviation. Tests were performed 10 times for each state. AD air-dried, OD oven-dried

Fourier-transformed infrared spectra

The FTIR spectra from birch bark are shown in Fig. 2. Untreated birch cork showed two strong peaks at 2929 and 2851 cm^{-1} (Fig. 2a, arrows). After suberin removal, intensity of the two peaks decreased significantly, and peaks at 1600 and 1510 cm^{-1} were observed (Fig. 2b, arrowheads). After delignification, these peaks almost disappeared (Fig. 2c).

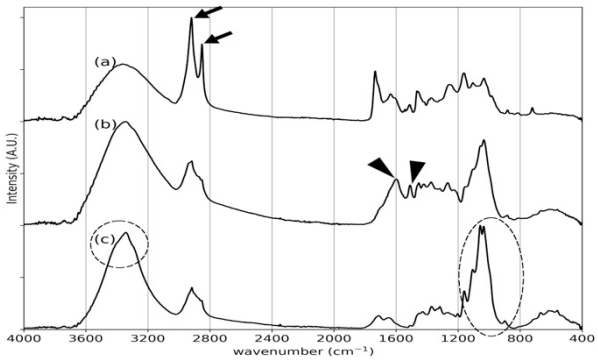

Fig. 2 Fourier-transformed infrared spectra of birch cork before chemical treatment (a), after removal of suberin (b), and after removal of suberin and lignin (c). Arrows indicate CH stretching peaks that stem from the suberin aliphatic domain. Arrowheads indicate peaks that stem from aromatic skeleton vibrations of lignin. Ellipses indicate the fingerprint region of cellulose I

Polarizing light microscopic observation

The PLM micrographs of radial sections from birch cork cell walls with and without degradation of suberin are shown in Fig. 3. Intact birch cork cell walls were yellow-colored (data not shown). Therefore, sections from samples without removal of suberin were also bleached using the Wise method to investigate molecular chain orientation from the polarization color. In radial sections, birch cork cells were from rectangular to hexagonal in shape elongated to longitudinal direction with an oval lumen. The proportion of lumen in the cells was larger in early cork than in late cork. Under open-Nicol condition, the cell wall showed a two-layer structure: thick outer layer, thin and oval-shaped inner layer. In addition, there was the inner material bordering cell wall (Fig. 3a). This layered structure was common to both early cork and late cork. In addition, the compound middle lamella and inner layer were strongly stained by the PAS reaction. Under cross-Nicol condition, the outer layer and inner material exhibited strong birefringence and inner material showed oval-shaped as like layer (Fig. 3b). Under a retardation plate, they showed a blue color in the tangential wall (Fig. 3c). After degradation of suberin, the outer layer and inner material disappeared, and the inner layer and compound middle lamella were

observed under open-Nicol condition (Fig. 3d). Under cross-Nicol condition, the compound middle lamella and inner layer exhibited weak birefringence (Fig. 3e). Under a retardation plate, the tangential wall of the compound middle lamella and inner layer showed a yellow color (Fig. 3f). The inner layers of early cork lost their shape whereas those of late cork remained oval shape by degradation of suberin (Fig. 3e-f).

The PLM micrographs of transverse sections from birch cork cell walls with and without degradation of suberin are shown in Fig. 4. Birch cork cells were elongated in tangential directions (Fig. 4). Under cross-Nicol condition, the outer layer and inner material exhibited strong birefringence (Fig. 4b). Under a retardation plate, the outer layer and inner material showed a yellow color in the tangential wall. After removal of suberin, it was difficult to distinguish which layer remained under open-Nicol condition (Fig. 4d). Under cross-Nicol condition, the remaining cell wall barely showed birefringence (Fig. 4e). Under a retardation plate, the tangential wall of the remaining cell wall showed a faint yellow color (Fig. 4f).

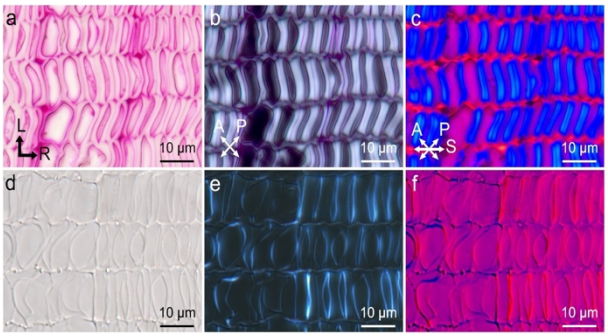

Fig. 3 Polarizing light micrographs of radial sections from birch cork stained by the periodic acid–Schiff reaction after bleaching using the Wise method (a–c), and unstained but subject to removal of suberin and lignin (d–f). Sections were observed under open-Nicol (a, d), cross-Nicol (b, e), and cross-Nicol condition with a retardation plate (c, f). L longitudinal direction, R radial direction, A analyzer, P polarizer, S slow axis

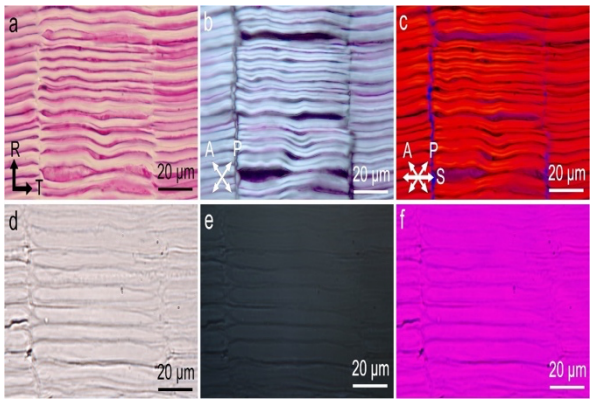

Fig. 4 Polarizing light micrographs of transverse sections from birch cork stained by the periodic acid–Schiff reaction after bleaching using the Wise method (a–c), and unstained but subject to removal of suberin and lignin (d–f). Sections were observed under open-Nicol (a, d), cross-Nicol (b, e), and cross-Nicol condition with a retardation plate (c, f). R radial direction, T tangential direction, A analyzer, P polarizer, S slow axis

Transmission electron microscopic observation

The TEM micrographs taken from $KMnO_4$-stained samples are shown in Fig. 5. In TEM observation, birch cork cell wall showed two-layered structure thick outer layer, thin and oval-shaped inner layer, and the inner material bordering cell wall showed amorphous shape. In the sections stained after resin embedding, the compound middle lamella, inner layer, and inner material were stained with $KMnO_4$ (Fig. 5a, d–f). The inner layer was oval-shaped in radial section (Fig. 5a) and pointed in the longitudinal and tangential directions (Fig. 5a, e). In the samples stained before Spurr's resin embedding, only the inner material was stained and the inner layer showed a lower electronic density than the outer layer (Fig. 5b). In the sample embedded in Epon812 resin after removal of suberin and lignin, the area other than the inner layer and compound middle lamella was stained with $KMnO_4$ (Fig. 5c).

The TEM micrographs captured from OsO_4-stained samples are shown in Fig. 6. Alternating layers of electron-dense and electron-lucent areas were observed in the outer layers of both early cork and late cork (Fig. 6a, d). The inner material appeared thinner in early cork than in late cork (Fig. 6a, d).

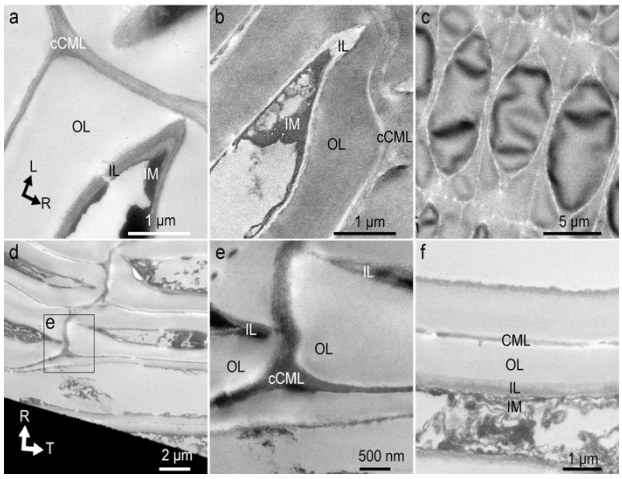

Fig. 5 Transmission electron micrographs of $KMnO_4$-stained radial (a–c) and transverse (d–f) sections. Staining was performed before embedding with Spurr resin (b), after embedding with Spurr resin (a, d–f), or after removal of suberin and lignin, and Epon812 resin embedding (c). cCML corner of compound middle lamellae, CML compound middle lamella, OL outer layer, IL inner layer, IM inner material bordering cell wall, L longitudinal direction, R radial direction, T tangential direction

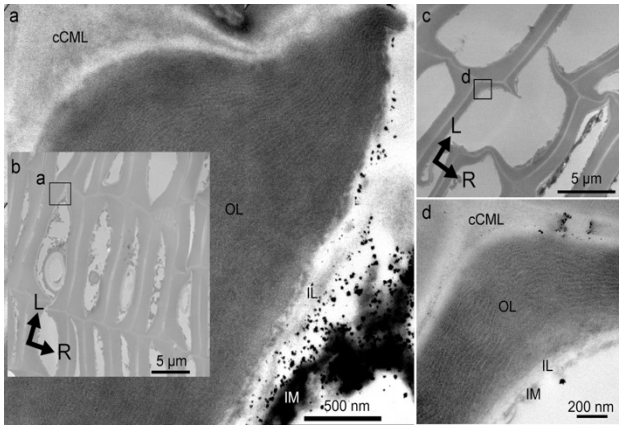

Fig. 6 Transmission electron micrographs of OsO_4-stained radial section cut from late cork (a, b) and early cork (c, d). Staining was performed before embedding. cCML corner of compound middle lamellae, CML compound middle lamella, OL outer layer, IL inner layer, IM inner material bordering cell wall, L longitudinal direction, R radial direction

Raman microscopic observation

Raman spectra obtained from birch cork cell walls are shown in Fig. 7. Spectra were obtained from the outer part of the cell wall (Fig. 7c) and inner material bordering cell wall (Fig. 7d). Both spectra included two strong CH stretching bands at 2929 and 2851 cm^{-1} (Fig. 7a, b). Spectra from the outer wall showed a weak OH stretching vibration at 3440 cm^{-1} (Fig. 7a). Bands at 1600 cm^{-1} and 1640 cm^{-1} were slightly stronger in the inner material than in the outer wall (Fig. 7a, b).

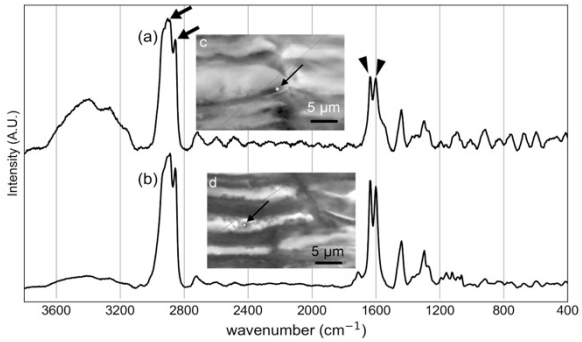

Fig. 7 Raman spectra (a, b) of birch cork acquired from the point indicated by arrows in brightfield micrographs (c, d) of a transverse section. Arrows in (a) indicate CH stretching bands that stem from the suberin aliphatic domain. Arrowheads indicate peaks that stem from the aromatic ring.

Discussion

Chemical composition and architecture of birch cork cell wall

The FTIR spectrum of untreated birch cork showed a similar pattern to those of Prunus serrula and Quercus suber (Xu et al. 1997). Two sharp CH stretching peaks at 2929 and 2851 cm^{-1} (Fig. 2a, arrows) were considered to stem from the suberin aliphatic domain. Two peaks at 1600 and 1510 cm^{-1}, which appeared after removal of suberin by alkali ethanolysis (Fig. 2b, arrowheads), originated from aromatic skeleton vibrations of lignin. After delignification using the Wise method, these peaks disappeared and the spectrum clearly showed the fingerprint region of cellulose I crystals (Fig. 2c, ellipses). Therefore, it was confirmed that these chemical treatments successfully removed suberin and lignin and that micrographs after treatment (Figs. 3d–f, 4d–f, and 5c) indicated observation of cellulose in the birch cork cell wall.

Both PLM and TEM micrographs indicated that the birch cork cell wall has a two-layered structure (Figs. 3, 5, and 6). In the OsO4-stained samples, the outer layer showed a multilayered structure with alternating electron-dense and -lucent layers (Fig. 6a, c). This pattern is typical of a suberized cell wall, as

reported previously (Ryser and Holloway 1985; Serra et al. 2009; Sitte 1962; Teixeira and Pereira 2010). Therefore, birefringence in the outer wall is considered to originate from the aliphatic domain of suberin. The PLM observation with a retardation plate showed that the suberin aliphatic domain of the outer layer and inner material is oriented perpendicular to the suberin lamella observed in TEM micrographs. These results agreed with previous reports indicating that the electron-lucent layers correspond to the aliphatic domain of suberin and that the molecular chain of the domain is oriented perpendicular to the suberin lamella (Schmutz et al. 1993, 1996).

The compound middle lamella and inner layer were strongly stained by the PAS reaction (Fig. 3a) and $KMnO_4$ (Fig. 5a–d). These observations indicated the presence of lignin and other polysaccharides. In the samples embedded in Epon812 resin after removal of suberin and lignin, $KMnO_4$ stained parts of the cell wall other than the compound middle lamella and inner layer (Fig. 5f). Previously, $KMnO_4$ was reported to stain methyl nadic anhydride of Epon812 resin (Reedy 1965). As mentioned above, the main component of the residue after removal of suberin and lignin is cellulose. Therefore, birefringence in PLM micrographs after the chemical treatments (Figs. 3d–f and 4d–f) indicated the orientation of cellulose microfibrils. The PLM observation with a retardation plate showed that cellulose microfibrils in the inner layer are oriented in the longitudinal direction of the tree body.

The inner material was stained with OsO_4 similar to the outer layer (Fig. 6). However, the inner material was stained also with $KMnO_4$, whereas the outer wall was barely stained (Fig. 5). These results implied the presence of a free phenolic hydroxyl group, which is reportedly stained with $KMnO_4$ (Bland et al. 1971). In the samples stained en bloc before embedding, only the inner material was stained (Fig. 5e). This may suggest that the inner material acts as a hydrophobic barrier between the lumen and inner layer. Raman spectra obtained from the outer and inner parts of the cork cell wall showed similar patterns (Fig. 7a, b). However, the spectrum from the outer part showed weak and broad bands at 3430 cm^{-1} and bands at 1600 and 1640 cm^{-1} were slightly stronger in the inner part than in the outer part. Bands at 3430 cm^{-1} in the outer cell wall were derived from cellulose in the compound middle lamella. Stronger peak intensity at 1600 and 1640 cm^{-1} in the inner material was considered to be aromatic and phenolic compounds. These results suggested that the inner material contained not only suberin but also phenolic compounds. The inner material showed oval shape bordering inner layer and lumen under cross-Nicol condition though it was amorphous like in TEM images (Figs. 3b and 5). It indicates that aliphatic chains of the inner material are arranged regularly as like those of outer layer.

Tensile properties and cell wall components of birch bark

The tensile tests revealed that birch cork in the wet state showed significantly higher extensibility than in the air-dried and oven-dried states. Birch cork showed a higher elastic modulus in the air-dried and oven-dried states than in the wet state. Note that significant decrease in toughness did not occur in the air-dried state but occurred in the oven-dried state. These results indicated that water plays an important role in stress transfer of birch cork in the tangential direction and, therefore, stress concentration occurs in the dried state. However, suberin, which is the predominant component of the cork cell wall, is highly hydrophobic and is unlikely to interact with water. Therefore, it is reasonable to imagine that the inner layer and compound middle lamella are engaged in bearing tensile stress and stress-transfer between cells. Kobayashi et al. (2018) performed tensile tests of cherry cork and investigated the molecular orientation under tensile load in cherry cork with X-ray diffraction. From the experimental results, they proposed a hierarchical model of cherry cork cell wall. Here, birch cork showed similar tensile behavior to that of cherry cork in air-dried state. Birch cork has inner material bordering cell wall in addition

to two-layered cell wall like that of cherry cork cell wall. Based on the structural model from the previous report and the present observations, we slightly modified a hierarchical model for the birch cork cell wall, where the lignified layer with a helical arrangement of cellulose microfibrils is covered with outer layer and lined with inner material as in Fig 8. The outer layer and inner material are suberized, and molecular chains of the suberin aliphatic domains are oriented perpendicular to the suberin lamellae. Under tensile stress in the tangential direction, cellulose microfibrils in the inner layer act like a spring and bear the tensile load. In the wet state, water and cellulose in the compound middle lamellae transfer tensile stress between cells, thus forming a tandemly connected spring. In the dried state, this stress-transferal system does not function well and fewer cells are engaged to bear stress. This results in lower extensibility in the dried state than that in the wet state (Fig. 1). Suberin in the outer layer and inner material may prevent cellulose in the inner layer and compound middle lamella from losing water so that the bark can bear tensile stress caused by trunk diameter growth. In addition, birch cork showed as much as 70% of extensibility in oven-dried state. This is significantly larger value than that of oven-dried cherry cork reported by Kobayashi et al. (2018). Inner material, which cherry cork does not have, may play an important role in maintaining mechanical properties of birch cork to some extent even after severe oven-drying.

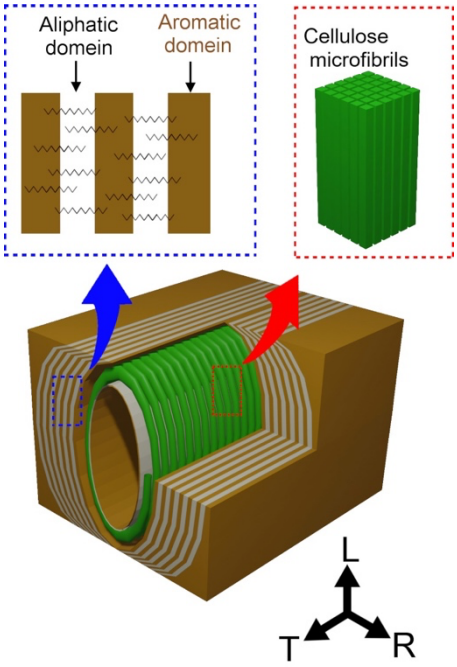

Fig. 8 Schematic illustration of the birch cork cell wall. L longitudinal direction, R radial direction, T tangential direction.

Comparison of properties between birch and cherry cork

In air-dried state, as mentioned above, birch cork shows similar tensile behavior to that of cherry cork reported in previous research (Kobayashi et al. 2018; Xu et al. 1997). This is due to the tangentially elongated cell shape of both birch and cherry cork. However, the tensile strength and toughness of birch cork is lower than that of cherry cork. This can be explained by the larger lumen and thinner cellulosic layer of birch cork compared with those of cherry cork. The larger lumen may result in higher insulation from low temperature. In addition, as mentioned above, the deterioration of tensile properties caused by oven-drying was less significant in birch cork. These may be parts of many reasons for the widespread distribution of birch on the Eurasian continent. Of course, effects of other factors such as the presence of betulin should be investigated in the future research.

Role division of early and late cork

In microscopic observations, cell walls of early

and late cork showed similar layered structures, molecular orientation, and histochemical staining patterns (Figs. 3, 4, 5, and 6). They differ in cell shape. Early cork showed apparently lager lumen than late cork (Figs. 3 and 6). On the other hand, late cork has thicker cell wall (Fig. 6). In addition, inner layers of late cork remained oval shape even after degradation of suberin and lignin (Fig. 3e-f). These observations indicate that early cork mainly plays a role of thermal insulating material, whereas late cork plays a role of mechanical strength of cork.

Conclusions

This research investigated the histochemical structure and tensile properties in the tangential direction of birch cork. The birch cork cell wall has a two-layered structure and inner material bordering cell wall. The thick outer layer and the amorphous like inner material predominantly consist of suberin. The inner layer mainly consists of lignin, cellulose, and other polysaccharides. Tensile tests indicated that birch cork in the wet and air-dried states show higher extensibility and toughness than that in the oven-dried state. These results indicate that cellulose in the inner layer bears tensile loads and that water in the inner layer and compound middle lamella plays an important role in the stress-transferal mechanism. The suberized outer layer and inner material may act as hydrophobic barriers and prevent complete water loss to maintain the tensile properties of cork.

Acknowledgements

This research was financially supported by Grants-in-Aid for Scientific Research on Innovative Areas (18H05485). The TEM observation was performed in collaboration with the Analysis and Development System for Advanced Materials (ADAM) at the Research Institute for Sustainable Humanosphere, Kyoto University. We thank Robert McKenzie, PhD, from the Edanz Group (https://en-author-services.edanz.com/ac) for editing a draft of this manuscript.

Declarations

Conflicts of interest

The authors declare that they have no conflict of interest.

Human and Animal rights

Not applicable.

References

Anjos O, Pereira H, Rosa ME (2008) Relation between mechanical properties of cork from Quercus Suber. II LATIN AMERICAN IUFRO CONGRESS. La Serena, Chile - Octubre 23-27.

Anjos O, Pereira H, Rosa ME (2010) Tensile properties of cork in the tangential direction: variation with quality, porosity, density and radial position in the cork plank. Materials and Design 31:2085-2090

Bhat KM. 1982. Anatomy, basic density and shrinkage of birch bark. IAWA Bull. n.s. 3:207-213

Ekman R, Eckerman C (1985) Aliphatic carboxylic acids from suberin in birch outer bark by hydrolysis, methanolysis and alkali fusion. Paperi ja Puu. 67:255-273.

Gandini A, Neto CP, Silvestre AJD (2006) Suberin: A promising renewable resource for novel macromolecular materials. Prog. Polym. Sci. 31:878-892

Gibson LJ, Easterling KE, Ash MF (1981) The structure and mechanics of cork. Proc. R. Soc. Lond. 377:99-117

Kobayashi K, Ura Y, Kimura S, Sugiyama J (2018) Outstanding toughness of cherry bark achieved by helical spring structure of rigid cellulose fiber combined with flexible layers of lipid polymers. Adv. Mater. 30:1705315

Pereira H (2015) The rationale behind cork properties: A review of structure and chemistry. Bioresources 10:6207-6229

Reedy MK (1965) Section staining for electron microscopy. Incompatibility of methyl nadic anhydride with permanganates. J. Cell Biol. 26:309-11

Ryser U, Holloway PJ (1985) Ultrastructure and chemistry of soluble and polymeric lipids in cell walls from seed coats and fibres of Gossypium species. Planta 163:151-163

Schmutz A, Jenny T, Amrhein N, Ryser U (1993) Caffeic acid and glycerol are constituents of the suberin layers in green cotton fibres. Planta 189:453-460

Schmutz A, Buchala AJ, Ryser U (1996) Changing the dimensions of suberin lamellae of green cotton fibers with a specific inhibitor of the endoplasmic reticulum-associated fatty acid elongases. Plant Physiol. 11:403-411

Schönherr J, Ziegler H. 1980. Water permeability of Betula periderm. Planta 147: 345-354

Serra O, Soler M, Hohn C, Sauveplane V, Pinot F, Franke R, Schreiber L, Prat S, Molinas M, Figueras M (2009) CYP86A33-targeted gene silencing in potato tuber alters suberin composition, distorts suberin lamellae, and impairs the periderm's water barrier function. Plant Physiol. 149:1050–1060

Shibui H, Sano Y (2018) Structure and formation of phellem of Betula maximowicziana IAWA J. 39:18-36

Sitte P (1962) Zum Feinbau der Suberinschichten im Flaschenkork. Protoplasma. 54:555-559

Teixeira RT, Pereira H (2010) Suberized cell walls of cork from cork oak differ from other species. Microsc. Microanal. 16, 569–575,

Xu X, Schneider E, Chien AT, Wudl F (1997) Nature's high-strength semitransparent film: The remarkable mechanical properties of Prunus Serrula bark. Chem. Mater. 9:1906-1908

Yang YP, Zhang Y, Lang YX, Yu MH (2017) Structural ATR-IR analysis of cellulose fibers prepared from a NaOH complex aqueous solution. IOP Conf. Series: Materials Science and Engineering 213:012039

Zhang X, Chen S, Ling Z, Zhou X, Ding DY, Kim YS, Xu F (2016) Method for removing spectral contaminants to improve analysis of raman imaging data. Scientific Reports 7:39891